

OPEN

Multidecade Mortality and a Homolog of Hepatitis C Virus in Bald Eagles (*Haliaeetus leucocephalus*), the National Bird of the USA

Tony L. Goldberg^{1,2*}, Samuel D. Sibley¹, Marie E. Pinkerton¹, Christopher D. Dunn¹, Lindsey J. Long³, LeAnn C. White⁴ & Sean M. Strom³

The bald eagle (*Haliaeetus leucocephalus*) once experienced near-extinction but has since rebounded. For decades, bald eagles near the Wisconsin River, USA, have experienced a lethal syndrome with characteristic clinical and pathological features but unknown etiology. Here, we describe a novel hepacivirus-like virus (*Flaviviridae: Hepacivirus*) identified during an investigation of Wisconsin River eagle syndrome (WRES). Bald eagle hepacivirus (BeHV) belongs to a divergent clade of avian viruses that share features with members of the genera *Hepacivirus* and *Pegivirus*. BeHV infected 31.9% of eagles spanning 4,254 km of the coterminous USA, with negative strand viral RNA demonstrating active replication in liver tissues. Eagles from Wisconsin were approximately 10-fold more likely to be infected than eagles from elsewhere. Eagle mitochondrial DNA sequences were homogeneous and geographically unstructured, likely reflecting a recent population bottleneck, whereas BeHV envelope gene sequences showed strong population genetic substructure and isolation by distance, suggesting localized transmission. Cophylogenetic analyses showed no congruity between eagles and their viruses, supporting horizontal rather than vertical transmission. These results expand our knowledge of the *Flaviviridae*, reveal a striking pattern of decoupled host/virus coevolution on a continental scale, and highlight knowledge gaps about health and conservation in even the most iconic of wildlife species.

For its majestic splendor, the bald eagle (*Haliaeetus leucocephalus*) was selected as the emblem of United States of America by the Continental Congress of 1782¹. For millennia prior, the bird was recognized as sacred by diverse Native American peoples². Despite its importance to North American histories and cultures, the bald eagle nearly went extinct in the 1960s due to eggshell thinning caused by dichlorodiphenyldichloroethylene (p,p'-DDE), a biodegradation product of dichlorodiphenyltrichloroethane (DDT)^{3,4}. The publication of Rachel Carson's *Silent Spring* in 1962⁵, subsequent banning of agricultural DDT use in the USA and Canada in the early 1970s⁶, and improved protections under the Bald and Golden Eagle Protection Act of 1940 and the Endangered Species Act of 1973^{7,8} helped the species recover from a nadir of 487 breeding pairs in the coterminous United States in 1963 to over 16,000 breeding pairs in 2009^{9–11}. The bald eagle was removed from the US federal list of threatened and endangered species in 2007⁷. Currently, major causes of bald eagle mortality, especially for birds living near people, include poisoning, trauma, electrocution, and illegal hunting^{12,13}.

Infections of bald eagles have been documented since the early 1900s but (with the possible exception of West Nile virus^{14,15}) have generally been considered sporadic and incidental^{10,12,16,17}. Among 2,980 bald eagle carcasses submitted to the U.S. Geological Survey National Wildlife Health Center (NWHC) in Madison, Wisconsin, USA, between 1982 and 2013, only 5.2% of deaths were attributed to infectious diseases¹². Documented infectious diseases of bald eagles include: ectoparasitoses^{18,19}, helminthoses^{20–24}, aspergillosis²⁵, coccidiosis²⁶, toxoplasmosis^{27–29}, sarcocystosis^{30–32}, leucocytozoonosis³³, avian malaria^{34–36}, avian cholera³⁷, mycobacteriosis^{38,39}, trichomoniasis⁴⁰, other bacterioses^{41–43}, avian pox⁴⁴, herpes⁴⁵, avian influenza^{46,47}, Newcastle disease⁴⁸, eastern equine encephalitis⁴⁹, and West Nile encephalitis¹⁵. However, many of these infections are known from only single cases

¹Department of Pathobiological Sciences, University of Wisconsin-Madison, Madison, WI, 53706, USA. ²Global Health Institute, University of Wisconsin-Madison, Madison, WI, 53706, USA. ³Wisconsin Department of Natural Resources, Madison, WI, 53707, USA. ⁴U.S. Geological Survey National Wildlife Health Center, Madison, WI, 53711, USA. *email: tony.goldberg@wisc.edu

or case clusters and affected birds often present with comorbidities, such that the importance of infection for bald eagle population health remains unclear.

Since approximately 1994, bald eagles near the lower Wisconsin River in Wisconsin, USA, have experienced a lethal and enigmatic clinical syndrome, Wisconsin River eagle syndrome (WRES)⁵⁰. WRES, which has not previously been described in the peer-reviewed literature, has been diagnosed in most years since its initial documentation, with mortality occurring between November and early April and peaking in January and February. Affected birds generally show good body condition, suggesting acute onset, and exhibit severe neurologic deficits (weakness, incoordination, tremors, vomiting and seizures). The condition is refractory to treatment, and death or euthanasia follow shortly. WRES is characterized by hepatocellular cytoplasmic vacuolation, with vasculitis and cerebral microhemorrhages sometimes observed. The neurologic signs and hepatic pathology characteristic of WRES initially led to investigations of potential toxic causes, but no suspect chemical compounds have been identified. Similarly, testing for known pathogens, including neurotropic viruses such as West Nile virus, has failed to identify an infectious etiology.

In an effort to identify the cause of WRES, we examined bald eagle tissues archived at the Wisconsin Department of Natural Resources and the NWHC. Submissions of carcasses to these agencies included cases from eagles in Wisconsin that had died of WRES as well as eagles from Wisconsin and across the coterminous USA that had putatively died from other causes. Given the known susceptibility of raptors to viral encephalitides (e.g. West Nile encephalitis⁴⁵) and the observation of neurologic signs and hepatic pathology in affected eagles, we investigated potential viral causes. Our analyses led to the identification of a novel hepacivirus-like virus (*Flaviviridae: Hepacivirus*), the type-virus of which is the globally important human pathogen hepatitis C virus (HCV)⁵¹. Herein we characterize the virus and describe our subsequent investigations into its distribution across the coterminous United States, its potential association with clinical disease, the population genetic structure of host and virus, and patterns of host-virus coevolution.

Results

Virus identification and characterization. Next-generation sequencing of reverse-transcribed RNA from tissues of nine bald eagles that had died of WRES revealed the presence of a novel virus, which we designated bald eagle hepacivirus (BeHV; GenBank accession number MN062427). The virus was identified in serum from a bird collected on December 29, 2002, from Sauk County, Wisconsin, and the bird displayed hepatocellular cytoplasmic vacuolation characteristic of WRES (Fig. 1). The 11,019 nucleotide coding-complete viral genome sequence contained a single, 3430 amino acid open reading frame and genomic features characteristic of members of the genus *Hepacivirus* within the family *Flaviviridae* (Fig. 2A), including a model Kozak sequence (AAGAUGG) at the proposed translation initiation site. Across the genome, BeHV is most similar to duck hepacivirus (DuHV⁵²) and generally more similar to HCV than to human pegivirus (HPgV), including immediately downstream of the E1/E2 junction, where homology between BeHV and other viruses is indiscernible (Fig. 2B). Similar to other members of the genus *Hepacivirus*, BeHV shows clear evidence of intrinsically disordered regions spanning the capsid protein and the 5' half of NS5A⁵³. Predicted cleavage sites are most conserved between BeHV and DuHV and show varying levels of conservation between BeHV and other hepaciviruses and pegiviruses (Fig. 2C). Phylogenetic analysis indicates that BeHV and DuHV form an avian lineage that is divergent with respect to the mammalian hepaciviruses and other hepacivirus-like viruses of non-mammalian hosts (Fig. 3). The mammalian hepaciviruses and the non-mammalian hepacivirus-like viruses together form a clade distinct from the pegiviruses (Fig. 3).

Nucleotide-level similarity within the 5'UTR, which has proven useful for inferring hepacivirus taxonomy and function^{54–56}, is low between BeHV and homologous regions of HCV (50.5%) and the human pegivirus HPgV (41.8%). Minimum free energy prediction of RNA secondary structure shows this portion of the BeHV 5'UTR to exhibit three large and well-defined stem-loop (SL) structures (Fig. S1). This predicted secondary structure more closely resembles that of the 5'UTR of HCV, a member of the genus *Hepacivirus*, than the 5'UTR of HPgV, a member of the genus *Pegivirus* (Fig. S1), and it also resembles that of rodent hepacivirus⁵⁶. However, the SL proximal to the polyprotein start codon lacks the obvious pseudoknot structure proposed for several hepaciviruses⁵⁷, and the BeHV internal ribosome entry site (IRES) more closely resembles those of certain pegiviruses, as has been noted for DuHV⁵².

Distribution of BeHV across the coterminous USA. Testing of 47 eagle liver tissues (which we chose to perform based on the known hepatic tropism of the hepaciviruses) from Wisconsin and elsewhere in the United States (Table S1) using metagenomics and nested rt-PCR revealed 14 additional samples to be positive for BeHV. Overall, 15/47 (31.9%) eagle liver samples were positive for BeHV, and these were collected from seven states (KS, FL, MN, ND, NE, WA and WI) out of 19 states where samples were available, with infections spanning 4,254 km of the coterminous United States (Table S1). Nested rt-PCR targeting negative-strand BeHV RNA produced amplicons of the expected size, which we confirmed by Sanger sequencing, indicating active viral replication in liver tissues.

Real time quantitative reverse transcription PCR (RT-qPCR) of RNA from liver tissues of the 15 BeHV-positive eagles yielded Ct values ranging from 26.1 to 36.4, with an overall mean of 30.26 (Fig. S2). Ct values from liver tissues of eagles from Wisconsin (Table S1) were not statistically different from Ct values of liver tissues from eagles from elsewhere (Fig. S2). The eagle in which we originally detected BeHV had a Ct value of 31.9, which was within the range of Ct values of other positive eagles (Fig. S2).

Between 1995 and 2018, the NWHC received 1188 bald eagle submissions, of which 260 (21.9%) were from Wisconsin. Of the 260 eagle submissions from Wisconsin, 28 (10.8%) were diagnosed clinically and histopathologically with WRES. No cases of WRES were diagnosed outside of Wisconsin. Of the 28 eagles diagnosed with WRES in Wisconsin, 14 (50.0%) came from counties bordering the lower Wisconsin River. Based on molecular

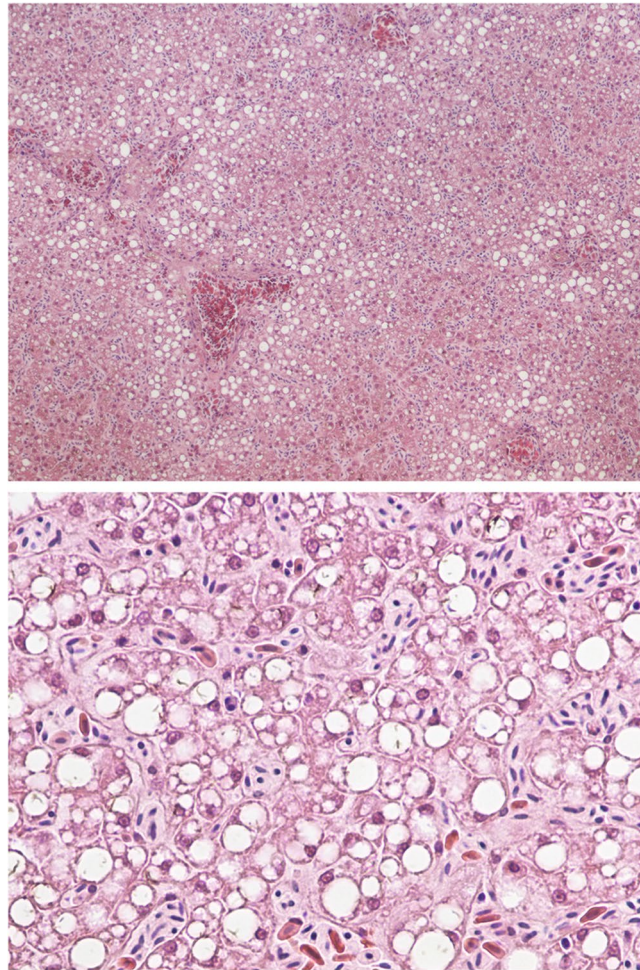


Figure 1. Liver from a bald eagle that died from Wisconsin River eagle syndrome stained with hematoxylin and eosin at 100x magnification (top) and 400x magnification (bottom), showing diffuse hepatocellular cytoplasmic vacuolation characteristic of this condition.

testing of tissues from 47 eagles (described above), the prevalence of BeHV in Wisconsin was 75.0% (95% confidence interval 40.1–93.7%), whereas the prevalence of BeHV elsewhere was 23.1% (95% confidence interval 12.4–38.5%), making eagles from Wisconsin 9.4 times more likely to test positive for BeHV than eagles from elsewhere (odds ratio = 9.406, 95% confidence interval 1.684–77.79; Fisher's exact $P=0.0086$). Similarly, the prevalence of BeHV in eagles from counties in Wisconsin where WRES had been diagnosed was 83.3% (95% confidence interval 41.8–98.9%), whereas the prevalence of BeHV in eagles from elsewhere was 24.4% (95% confidence interval 13.7–39.5%), making eagles from counties in Wisconsin where WRES had been diagnosed 14.5 times more likely to test positive for BeHV than eagles from elsewhere (odds ratio = 14.470, 95% confidence interval 1.782–378.80; Fisher's exact $P=0.0188$).

Host and virus population genetics and coevolution. Nucleotide-level genetic diversity (\pm standard error) among eagle mitochondrial DNA sequences (GenBank accession numbers MN062428–MN062562) was low ($\pi=1.03 \times 10^{-3} \pm 2.35 \times 10^{-4}$). Nucleotide level genetic diversity among virus envelope gene sequences from those same eagles (GenBank accession numbers MN062563–MN062576) was higher ($\pi=4.61 \times 10^{-2} \pm 3.43 \times 10^{-3}$). Analysis of isolation-by-distance revealed different patterns for hosts and viruses (Fig. 4). Mantel tests of matrix correlation indicated no statistically significant correlation between geographic and genetic distances for eagle mitochondrial DNA sequences ($r=0.120$; 2-tailed P value = 0.254) but a strong and statistically significant positive correlation between geographic and genetic distances for envelope gene sequences of viruses infecting those same eagles ($r=0.771$; 2-tailed P value < 0.0001). Virus pairs tended to sort into clusters of genetic similarity at discrete classes of geographic separation, revealing a spatial signal of viral population genetic substructuring across the coterminous USA that was not evident in eagle hosts (Fig. 4).

Phylogenetic analyses of eagle mitochondrial DNA sequences and virus envelope gene sequences yielded different topologies (Fig. 5). Maximum likelihood cladograms (Fig. 5, bottom) were inferred from an 8,266-position alignment of concatenated mitochondrial gene sequences of eagles and a 1,395-position alignment of envelope gene sequences of viruses using the same methods described for Fig. 3. Eagle sequences showed no apparent phylogeographic pattern and branch lengths were short, whereas viral sequences showed evidence of phylogeographic

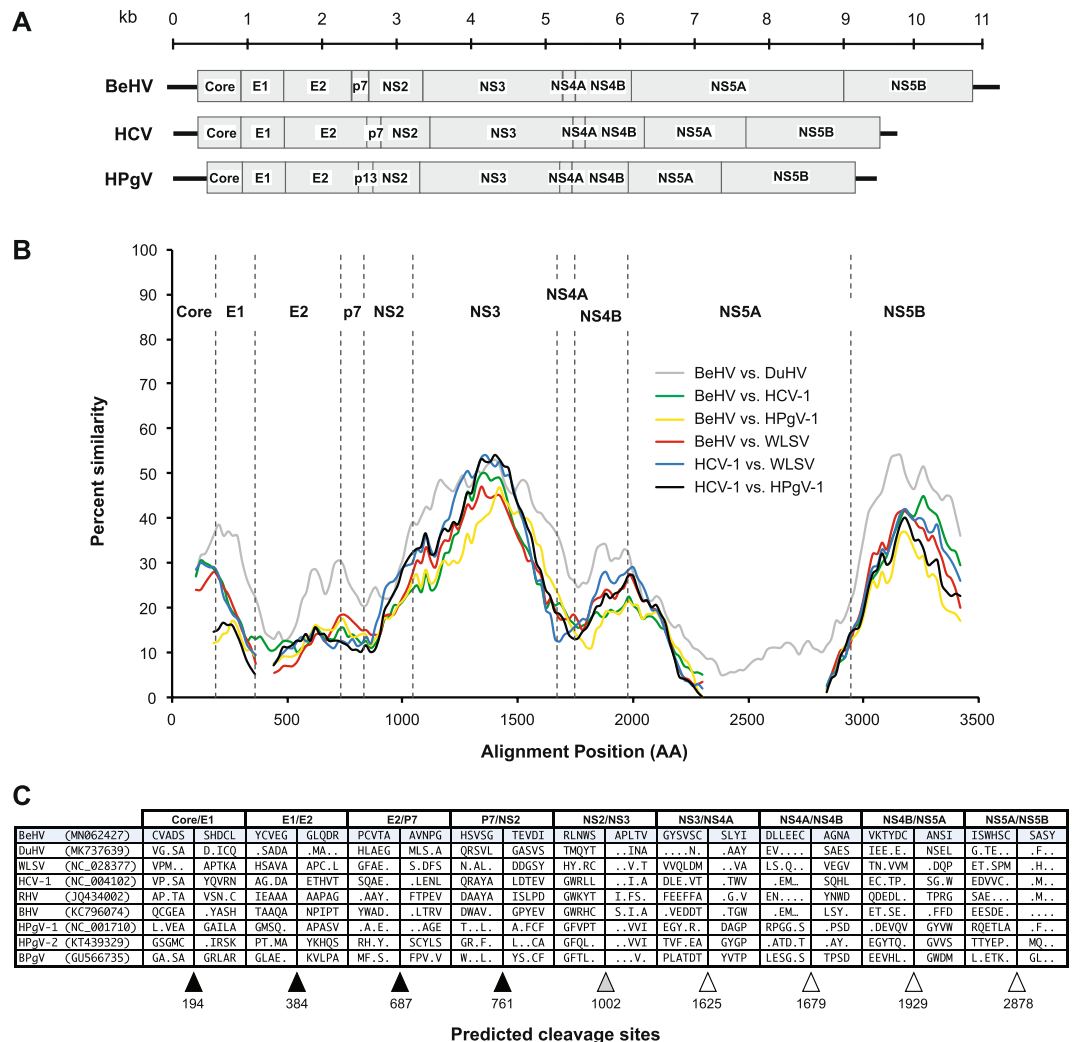


Figure 2. Genome organization, amino acid similarity, and polyprotein cleavage sites of bald eagle hepacivirus (BeHV) and related viruses. **A)** Genomic organization of BeHV, hepatitis C virus (HCV, the type virus of the genus *Hepacivirus*), and human pegivirus (HPgV; the type virus of the genus *Pegivirus*). Boxes represent mature proteins and are drawn to scale, and lines adjacent to core and NS5B proteins represent untranslated regions (UTRs). **B)** Sliding-window similarity plots across aligned amino acid sequences showing comparisons among BeHV, duck hepacivirus (DuHV), hepatitis C virus 1 (HCV-1), Wenling shark virus (WLSV), and human pegivirus 1 (HPgV-1). Dashed vertical lines indicate start positions of inferred viral proteins. **C)** Amino acid sequences of BeHV and related viruses adjacent to protease cleavage sites inferred using bioinformatic prediction. Predicted cleavage sites for signalase (black triangles), NS2-NS3 protease (gray triangle), and NS3-NS4A protease (white triangles) are indicated. Amino acid positions of cleavage sites in relation to BeHV are shown below the triangles.

clustering (e.g. viral sister taxa B and G and the clade consisting of viruses K, N and O) and branch lengths were longer (Fig. 5). Cophylogenetic analyses (Fig. 5) showed virus/host pair N and O to be sister taxa and virus/host pair A and B to be closely related in both phylogenies, but analysis of cophylogenetic association using the AxParafit algorithm⁵⁸ with 99999 permutations revealed no statistically significant overall cophylogenetic structure between eagle and virus phylogenies ($P = 0.139$) and only one statistically significant individual association (between host/virus pairs N and O; $P = 0.013$).

Discussion

Bald eagles are an iconic North American wildlife species that has faced myriad challenges. In the 1960s, bald eagles were nearly extirpated from the coterminous USA due to the toxic effects of DDT^{3,4}. Banning of DDT in the 1970s⁶ and improved Federal protections^{7,8} allowed the species to rebound, but eagles still experience significant mortality from anthropogenic factors such as poisoning, illegal hunting, trauma, habitat loss, and antagonistic interactions with people¹². Our results highlight two additional factors that have received comparatively little attention with respect to bald eagle conservation: infectious disease and lack of genetic diversity. We describe a novel hepacivirus-like virus, bald eagle hepacivirus (BeHV), discovered during an investigation into Wisconsin

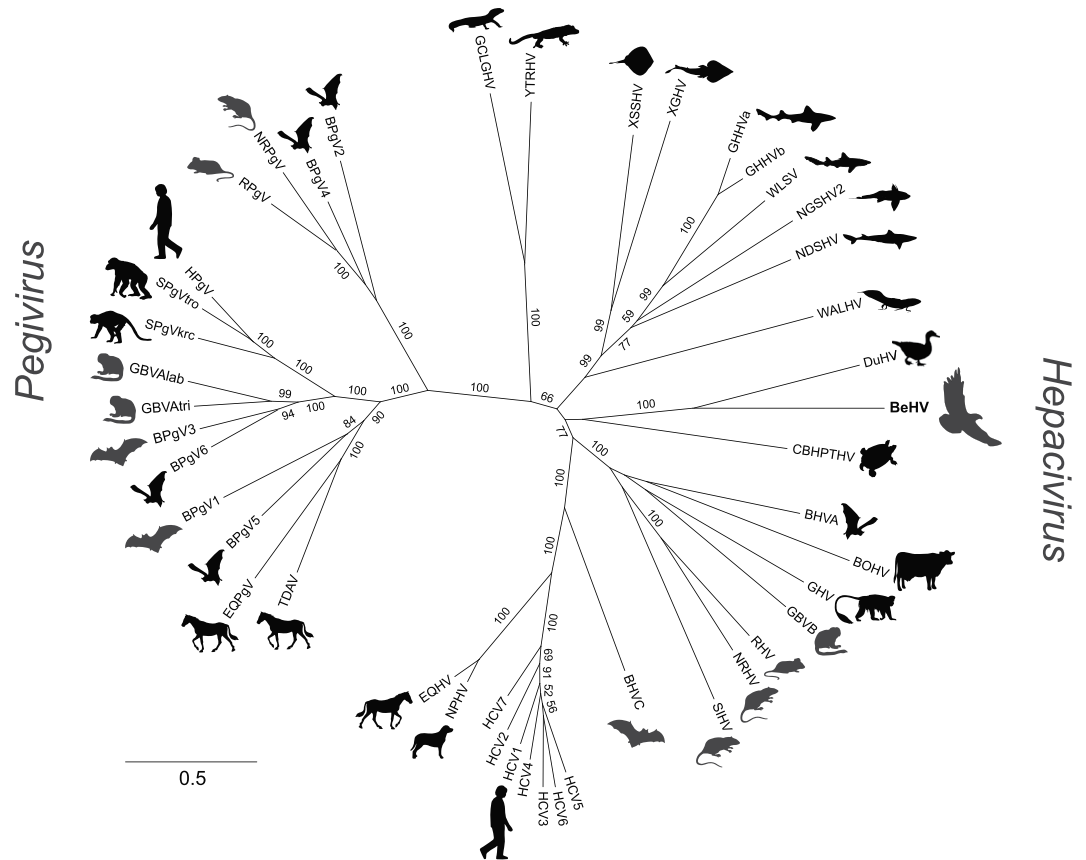


Figure 3. Maximum likelihood phylogenetic tree of hepaciviruses and pegiviruses, Silhouettes indicate the host in which each virus was originally described (right-facing for hepaciviruses and left-facing for pegiviruses); full virus names and GenBank accession numbers are given in Table S3. Numbers beside nodes indicate statistical confidence (percent) based on 1,000 bootstrap replicates of the data (only values $\geq 50\%$ are shown); scale bar indicates nucleotide substitutions per site.

River eagle syndrome, a lethal affliction of bald eagles. We also document remarkably low genetic diversity in bald eagles across the coterminous United States, consistent with the species' recent recovery from a population bottleneck^{11,59}.

We discovered BeHV during an attempt to determine the cause of WRES, which has defied etiologic diagnosis for decades⁵⁰, but the role of the virus in clinical disease remains uncertain. We identified the virus in the serum of a single affected eagle, but we did not find BeHV in this bird's brain tissue or in serum or brain tissues from eight other eagles that had died of WRES. We also found BeHV in 31.9% of eagle liver samples from across the USA. BeHV viremia is therefore likely transient or intermittent, and the site of persistence is probably the liver, as is characteristic of hepaciviruses⁵¹. Our initial analyses focused on brain and serum were therefore based on erroneous assumptions that a neurotropic virus was involved in WRES, because of the neurologic signs observed in many affected birds⁵⁰.

Loss of liver function can lead to hepatic encephalopathy, or accumulation of neurotoxic substances and their metabolites, which can cause severe neurologic deficits^{60–62}. Outwardly, the liver pathology characteristic of many WRES-affected eagles (e.g. Fig. 1) resembles that in human patients with chronic HCV infection⁶³. Cytoplasmic vacuolation in general often follows exposure to viral pathogens⁶⁴, although this lesion is inherently non-specific and can result from non-viral causes as well. Negative-strand RT-PCR demonstrated that BeHV actively replicates in liver tissues of infected birds, but we were unable to determine whether the virus was localized at the site of hepatocellular cytoplasmic vacuolation because our attempts to use RNAscope technology⁶⁵ to visualize BeHV in eagle livers failed due to the sub-optimal preservation conditions of field-collected specimens. Experimental infections of eagles or a suitable surrogate avian species will likely be necessary to determine the tropism of BeHV and to clarify its role in pathology and clinical disease.

We documented BeHV infection in eagles across 4,254 km of the coterminous USA, as far apart as the states of Florida and Washington. We also documented that eagles sampled from Wisconsin were 9.4 times more likely to be infected with BeHV than eagles from elsewhere, and that eagles from counties in Wisconsin where WRES had been diagnosed were 14.5 times more likely to be infected with BeHV than eagles from elsewhere. In a sample of 1188 eagles submitted to the NWHC over 23 years, WRES was diagnosed only in eagles from Wisconsin. This apparent concentration of WRES in Wisconsin (especially in counties bordering the lower Wisconsin River) may indicate locally favorable conditions for transmission or, alternatively, reporting or diagnostic bias.

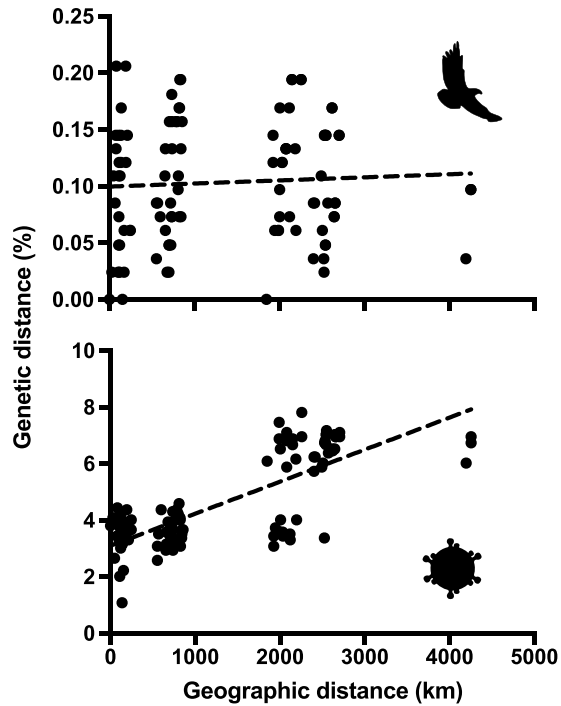


Figure 4. Isolation by distance for bald eagles and their viruses across the coterminous United States. Points indicate geographic-genetic distances between pairs of bald eagles (top) and bald eagle hepaciviruses (bottom); see Fig. 1 and Table S1 for details. Dashed lines are least squares regression lines.

Infections can weaken wildlife, making animals more vulnerable to other causes of mortality, such as predation, trauma, and starvation^{66,67}. BeHV could predispose eagles to such factors. If so, region-specific co-factors could interact with BeHV to precipitate particular disease manifestations. For example, parts of the lower Wisconsin River remain ice-free in Winter, providing eagles with rare fishing opportunities and creating dense aggregations of birds that attract tourists. Eagles could transmit infections under such circumstances¹⁴, and indeed WRES tends to strike in the Winter months⁵⁰. The same favorable conditions could also allow eagles to survive more readily to the end stages of infection, perhaps explaining the good body condition characteristic of WRES-affected eagles⁵⁰. Nevertheless, positive eagles from Wisconsin had viral loads no higher than those of birds from elsewhere. Unfortunately, our sample included only moribund or dead eagles submitted to state and federal agencies, which is not a representative sample of the population of eagles at large, such that additional effort will be required to ascertain whether BeHV is causally related to WRES in the wild.

Eagles showed no evidence of isolation by distance, as might be expected from their low genetic diversity likely resulting from bottleneck effects during their near-extinction in the 1960s⁵⁹ and their ability to fly long distances. By contrast, BeHV showed higher genetic diversity, strong evidence of isolation by distance, and distinct sorting of pairwise genetic distances into discrete geographic clusters (Fig. 4). Viral genomes (especially those of RNA viruses such as BeHV) evolve orders of magnitude more rapidly at the nucleotide sequence level than do vertebrate genes⁶⁸. Geographic substructuring of BeHV across the coterminous United States may therefore reflect population structure in bald eagles that is not yet evident in bald eagle genomes, such as might result from sub-specific or subpopulation differentiation related to migration and reproduction⁸. For example, viruses N, O and K in Fig. 4 are divergent from other viruses and also represent the only eagles analyzed from the Pacific flyway.

Eagle mitochondrial DNA and virus envelope gene sequence phylogenies were uncorrelated (Fig. 5). Because mitochondrial DNA is maternally inherited, this observation suggests that BeHV is not typically vertically transmitted. West Nile virus, another member of the family *Flaviviridae*, can be transmitted to bald eagles through feeding on infected prey and carrion, and perhaps directly from eagle to eagle, circumventing the normal vector-borne mode of transmission for this virus¹⁴. Bald eagles often congregate around food sources, especially in winter (when WRES most commonly occurs), where they interact aggressively with conspecifics and with other predatory birds during competition over carrion or prey items (“piracy”)^{69–71}, an aspect of their natural history that famously inspired Benjamin Franklin to impugn the species as “a bird of bad moral character”⁷¹. Such features of eagle social behavior could predispose them to cross-species and horizontal viral transmission. The reservoir of BeHV could be bald eagles, their prey/carrion, or other species with which they interact. Although no hepaciviruses are known to be vector-borne, this possibility should also not be discounted.

The family *Flaviviridae* currently contains four genera: *Flavivirus*, *Pestivirus*, *Pegivirus*, and *Hepacivirus*⁷². Members of the genus *Flavivirus* commonly infect birds (e.g. West Nile virus) and can cause lethal disease⁷³. The genus *Pestivirus* contains viruses that have so far only been found in mammals^{54,74,75}. The genus *Pegivirus*, also so far found only in mammals, contains an equine virus associated with Theiler’s disease of horses^{75–77} but no other known pathogens. HPgV is nevertheless of clinical interest because it may slow disease progression in patients

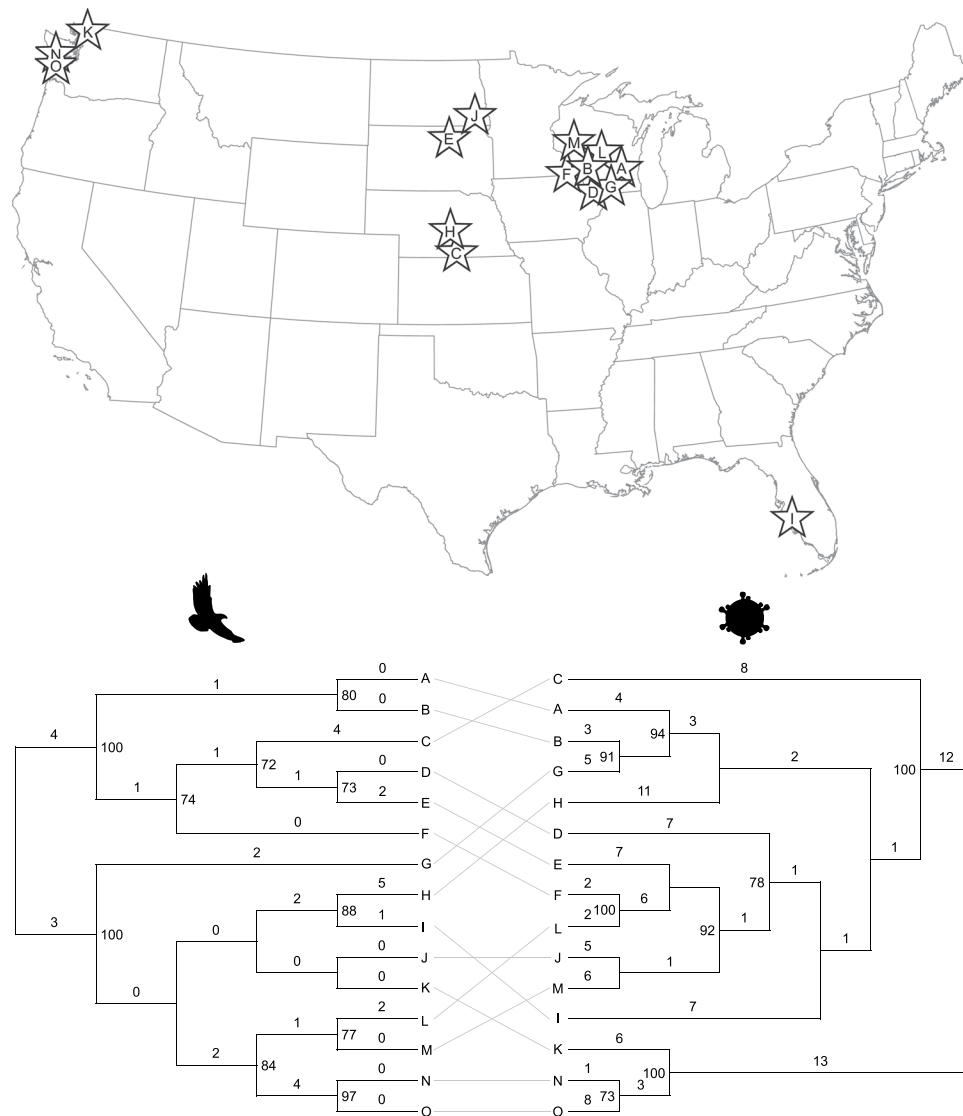


Figure 5. Geographic origins and cophylogenetic association of bald eagles and their viruses. Letters correspond to the locations from which eagles and their viruses were sampled, represented by stars on the map of the coterminous United States (top). For the tanglegram (bottom), numbers above branches indicate branch lengths (nucleotide substitutions per site $\times 10^{-4}$ for hosts and $\times 10^{-2}$ for viruses), and numbers beside nodes indicate bootstrap values based on 1000 bootstrap replicates of the data. Full information on eagles and viruses is given in Table S1.

with AIDS and Ebola virus disease through mechanisms that remain incompletely understood^{78,79}. Members of the genus *Hepacivirus* infect diverse mammals^{54,75,76}, and hepacivirus-like viruses have been found in reptiles, amphibians, fishes and domestic ducks^{52,54,80–82}. The hepaciviruses and pegiviruses are gaining recognition as examples of rapidly expanding viral genera that may hold important clues about the origins and pathogenesis of human and animal diseases alike^{54,75,80,81}.

Our results support the notion that the diversity and host range of the hepaciviruses will likely continue to expand. BeHV and DuHV form an avian lineage of hepacivirus-like viruses that also share genomic features with the pegiviruses, suggesting an undiscovered diversity of related avian viruses that may possess similar intriguing attributes. Across the genome, BeHV is more similar to the hepacivirus type virus (HCV) than to the pegivirus type virus (HPgV), suggesting a greater affinity of BeHV for the hepaciviruses than the pegiviruses. More broadly, our results show that the mammalian hepaciviruses form a sub-clade within a diverse clade of hepacivirus-like viruses from non-mammalian hosts, and the mammalian hepaciviruses and non-mammalian hepacivirus-like viruses form a clade distinct from the pegiviruses (Fig. 3). Taxonomic subdivision of the genus *Hepacivirus* may be necessary, especially if additional discoveries support the association of clades of hepacivirus-like viruses with particular host taxonomic groups (e.g. avian, amphibian, elasmobranch)⁷⁵.

Overall, our results show that bald eagles across the coterminous United States are infected with a novel hepacivirus-like virus that displays intriguing genomic features, epidemiologic patterns, and evolutionary history.

BeHV evolution and population genetics are strikingly decoupled from those of its host, perhaps reflecting a “lag effect” due to the recent recovery of eagles from a severe population bottleneck. The extent to which BeHV represents a threat to bald eagle health and conservation will require further investigation, as will determining its origin, reservoir(s) and mode(s) of transmission. Additional studies using expanded sample sets and associated clinical data from bald eagles and other birds should add to our understanding of BeHV and its relatives. Our findings already reveal how much remains to be discovered about health and conservation in North American wildlife, even in species central to the history and cultures of the continent.

Methods

Ethics statement and eagle tissues. We obtained bald eagle samples from tissue archives maintained by the NWHC and the WDNR from carcasses submitted post-mortem. We used the records system of the NWHC to obtain data on numbers of eagles submitted per year, their geographic origins, causes of death, and pathologic findings. Tissues were submitted, archived, and analyzed in accordance with all local, state, tribal, and federal laws and policies, and with appropriate permits. No live animals were used in this research.

Molecular methods. We processed serum and brain tissues from nine eagles that had died of WRES for deep sequencing and virus discovery as described previously^{83,84}. Briefly, we isolated viral nucleic acids using the QIAamp MinElute virus kit (Qiagen, Hilden, Germany), converted RNA to double-stranded cDNA using random hexamers, and prepared libraries for sequencing on an Illumina MiSeq instrument (V3 chemistry, 600 cycle kit; Illumina, San Diego, CA, USA) using the Nextera XT DNA sample preparation kit (Illumina, San Diego, CA, USA). We analyzed sequence data using CLC Genomics Workbench version 11.0 (CLC bio, Aarhus, Denmark), first trimming low-quality bases (phred quality score < 30) and discarding short reads (< 75 bp). We then analyzed unassembled reads and contiguous sequences derived from *de novo* assembly of raw reads for nucleotide-level (blastn) and protein-level (blastx) similarity to viruses in GenBank as previously described^{83,84}.

Based on the known hepatic tropism of the hepaciviruses, we next examined archived liver tissues of 47 birds (fresh frozen at -80°C), including the aforementioned juvenile eagle, of which eight were from Wisconsin (three of these from counties bordering the lower Wisconsin River) and 39 were from elsewhere (Table S1). From each sample, we collected 6 mm sterile punches (60 mg), suspended them in 1 mL of 1x Trizol in tubes with 2.38 mm metal beads (Qiagen, Hilden, Germany), and homogenized them in three 20-second cycles with a Mini-Beadbeater-96 instrument (Biospec Products, Bartlesville, OK). We then centrifuged the tubes at $12,000 \times g$ for 5 minutes at 4°C and supplemented 100 μL (~6 tissue equivalent) of supernatant with 900 μL of Trizol. We performed phase separation in 2 mL Phase Lock Gel Heavy tubes (5PRIME, Gaithersburg, MD) and purified nucleic acids from the aqueous phase using the RNA Clean & Concentrator-5 kit (Zymo Research, Irvine, CA). We then conducted deep sequencing as described above.

To test eagle liver samples for BeHV, we designed a nested RT-PCR using primers annealing to the highly conserved NTPase region of the viral NS3 gene (Table S2). We performed RT-PCR using the OneTaq RT-PCR kit (New England Biolabs, Ipswich, MA) followed by the KAPA HiFi HotStart PCR kit (KAPA Biosystems, Wilmington, MA). We included primers at 400 nM each and conducted RT-PCR as follows: 53°C for 30 minutes, 94°C for 2 minutes; 94°C for 15 s, 56°C for 30 s, and 68°C for 2.5 min for 40 cycles; and a terminal extension step at 68°C for 5 min. We then conducted 35 cycles of nested PCR using 1 μL of external PCR product as template and the same conditions described above, but omitting the initial reverse transcription step and with an annealing temperature of 58°C . We visualized amplicons on 2% agarose gels stained with ethidium bromide and purified them using the Zymoclean Gel DNA Recovery Kit (Zymo Research, Irvine, CA). We then prepared amplicons for sequencing using the Nextera XT DNA sample preparation kit (Illumina, San Diego, CA), followed by sequencing on an Illumina MiSeq (MiSeq Reagent Kit, v3, 150 cycles, Illumina, San Diego, CA).

To assess viral genetic variation, we amplified and sequenced the viral envelope gene in all positive tissues using nested RT-PCR assay (Table S1) and the same reagents described above. We included primers at 400 nM each and completed RT-PCR as follows: 50°C for 30 minutes, 94°C for 1 minute; 40 cycles of 94°C for 15 s, 56°C for 30 s, and 68°C for 1.5 min; and a terminal extension step at 68°C for 5 min. We conducted 35 cycles of nested PCR using 1 μL of external PCR product as template as described above, but omitting the initial reverse transcription step. We then visualized, purified, and sequenced PCR products as described above.

To assess eagle genetic variation and to provide host relatedness data for cophylogenetic analyses, we assembled sequences of 9 mitochondrial genes (control region, ND2, COX1, COX2, ATP6, COX3, ND4, ND5, and CYTB) from deep sequence data generated from liver tissues of all BeHV-positive eagles liver samples sequenced and analyzed as described above. We then concatenated the resulting sequences for population genetic and phylogenetic analyses.

To assess viral replication in liver tissues, we amplified negative-strand (replicative-intermediate) RNA following the methods of Lin *et al.*⁸⁵. We used the same primers, reagents and cycling conditions for nested RT-PCR described above, except that we appended the primer annealing to negative-strand RNA during reverse transcription (BeHV-NS3-EX-F3869) with a 5' blocking sequence (Table S2). During flanking RT-PCR, we added primer WRBEV-R4084 following reverse transcription and a reverse transcriptase inactivation step. We then used the 5' tag sequence (Table S2) as the forward primer and primer BeHV-R4017 as the reverse primer to preclude amplification of viral RNA that was either self-primed or primed by endogenous oligonucleotides during reverse transcription. We then verified amplicons by Sanger sequencing.

To assess relative viral loads, we conducted RT-qPCR using primers (Table S2) designed to anneal to regions conserved among all BeHV envelope gene sequences (determined as described above) and a ZEN double quenched probe (Integrated DNA Technologies, Coralville, IA). We ran reactions in triplicate on a BioRad CFX96 real-time system mounted on a C1000 thermocycler (BioRad, Hercules CA) using the GoTaq Probe 1-Step RT-qPCR System (Promega, Madison, WI) according to the manufacturer's recommendations, with 2 μL RNA

(extracted from 60 mg tissues, as described above) as input. We calculated viral loads as the Ct value averaged across three rtq-PCR replicates.

To visualize BeHV RNA *in situ*, we attempted to apply RNAscope technology⁶⁵ to histologic sections of eagle livers using RNAscope double “Z” oligonucleotide probes designed to hybridize to the BeHV polymerase gene; however, all attempts failed, likely because of the degraded nature of RNA in tissues from carcasses collected under field conditions.

Viral genome analyses. We determined the putative translation initiation codon for the BeHV open reading frame using the ATGpr prediction server⁸⁶, we used SignalP⁸⁷ to identify signal peptide sequences, and we used the IRESPred web server⁸⁸ to characterize the BeHV IRES. We also conducted analyses of core and NS5A protein sequences to identify intrinsically disordered regions (IDRs) and sites within IDRs with capacity to undergo disorder-to-order transitions for binding interactions using ANCHOR^{89,90}. Because of previous work showing that the 5′ untranslated region (UTR) of the hepaciviruses is informative for viral taxonomy and prediction of function⁵⁵, we analyzed homologous 3′ ends of this feature in BeHV, HCV and HPgV to predict RNA secondary structure using the mfold Web Server⁹¹ and the RNAfold algorithm executed on the Vienna RNA Websuite server^{92,93}.

Phylogenetic and evolutionary analyses. To infer the phylogenetic position of BeHV, we compiled nucleotide sequences of complete viral polyprotein genes available in Genbank representing known lineages within the hepaciviruses and pegiviruses. We then generated codon-based sequence alignments using the PRANK algorithm⁹⁴ with the Gblocks algorithm^{95,96} applied to remove poorly aligned regions using TranslatorX⁹⁷. We inferred phylogenies from the resulting 3,579-position nucleotide sequence alignment using PhyML⁹⁸, with the model of molecular evolution (GTR + Γ + I) estimated from the data⁹⁹ and 1,000 bootstrap replicates to assess statistical confidence in clades, and we displayed trees using FigTree¹⁰⁰. To compare BeHV and select hepacivirus-like viruses, hepaciviruses, and pegiviruses, we aligned full viral genomes as described above and examined variation in amino acid-level similarity across the length of the alignment using the sliding-window method implemented in SimPlot¹⁰¹.

To assess host and viral genetic diversity, we calculated nucleotide diversity (π)¹⁰² from aligned eagle and virus gene sequences using the computer program MEGA7¹⁰³. To assess isolation by distance, we computed pairwise geographic distances between centroids of the US county of origin from which each eagle was collected using Geographic Distance Matrix Generator¹⁰⁴. We then computed uncorrected pairwise genetic distances between eagles (mitochondrial gene sequences) and viruses (envelope gene sequences) and compared each to pairwise geographic distances using Mantel tests of matrix correlation¹⁰⁵ with 10,000 permutations of the data to assess statistical significance, implemented in the APE package in R¹⁰⁶.

To assess host-virus coevolution, we conducted cophylogenetic analyses. We generated codon-based sequence alignments of eagle concatenated mitochondrial DNA sequences and virus envelope gene sequences and inferred maximum likelihood phylogenies as described above. We then constructed tanglegrams using Dendroscope¹⁰⁷ and tested for overall phylogenetic congruence and the significance of individual host/virus associations using the AxParafit algorithm^{58,108} implemented in CopyCat, version 2.04¹⁰⁹.

Data availability

All data generated during the current study are available in GenBank (accession numbers MN062427–MN062576) or are included in this published article and its Supplementary Information files.

Received: 12 July 2019; Accepted: 12 September 2019;

Published online: 18 October 2019

References

1. Lawrence, E. A. Symbol of a nation: the bald eagle in American culture. *The Journal of American Culture* **13**, 63–69 (1990).
2. DeMeo, A. M. Access to eagles and eagle parts: environmental protection v. Native American free exercise of religion. *Hastings Constitutional Law Quarterly* **22**, 771–813 (1995).
3. Wiemeyer, S. N. *et al.* Organochlorine pesticide, polychlorobiphenyl, and mercury residues in bald eagle eggs—1969–79—and their relationships to shell thinning and reproduction. *Arch Environ Contam Toxicol* **13**, 529–549 (1984).
4. Bowerman, W. W., Giesy, J. P., Best, D. A. & Kramer, V. J. A review of factors affecting productivity of bald eagles in the Great Lakes region: implications for recovery. *Environ Health Perspect* **103**(Suppl 4), 51–59, <https://doi.org/10.1289/ehp.95103s451> (1995).
5. Carson, R. *Silent Spring*. 368 (Houghton Mifflin, 1962).
6. Kinkela, D. *DDT and the American Century: Global Health, Environmental Politics, and the Pesticide that Changed the World*. (University of North Carolina Press, 2011).
7. Stokstad, E. Can the bald eagle still soar after it is delisted? *Science* **316**, 1689–1690, <https://doi.org/10.1126/science.316.5832.1689> (2007).
8. Wright, K. R. Count trends for migratory Bald Eagles reveal differences between two populations at a spring site along the Lake Ontario shoreline. *PeerJ* **4**, e1986, <https://doi.org/10.7717/peerj.1986> (2016).
9. Grier, J. W. Ban of DDT and subsequent recovery of reproduction in bald eagles. *Science* **218**, 1232–1235 (1982).
10. Colborn, T. Epidemiology of Great Lakes bald eagles. *J Toxicol Environ Health* **33**, 395–453, <https://doi.org/10.1080/15287399109531537> (1991).
11. Millsap, B. A., Bjerre, E. R., Otto, M. C., Zimmerman, G. S. & Zimpfer, N. L. Bald and Golden Eagles: Population demographics and estimation of sustainable take in the United States, 2016 update. (U.S. Fish and Wildlife Service, Division of Migratory Bird Management, Washington D.C., USA., 2016).
12. Russell, R. E. & Franson, J. C. Causes of mortality in eagles submitted to the National Wildlife Health Center 1975–2013. *Wildl. Soc. Bull.* **38**, 697–704 (2014).

13. Dwyer, J. F., Sofi H. & Kratz, G. E. In *Urban Raptors: Ecology and Conservation of Birds of Prey in Cities* (eds Clint, W. B. & Cheryl, R. D.) 199–213 (Island Press, 2018).
14. Ip, H. S. *et al.* West Nile virus transmission in winter: the 2013 great salt lake bald eagle and eared grebes mortality event. *PLoS currents* **6**, doi:10.1371/currents.outbreaks.b0f031fc8db2a827d9da0f30f0766871 (2014).
15. Wunschmann, A. *et al.* Clinical, pathological, and immunohistochemical findings in bald eagles (*Haliaeetus leucocephalus*) and golden eagles (*Aquila chrysaetos*) naturally infected with West Nile virus. *J Vet Diagn Invest* **26**, 599–609, <https://doi.org/10.1177/1040638714539960> (2014).
16. Deem, S. L., Terrell, S. P. & Forrester, D. J. A retrospective study of morbidity and mortality of raptors in Florida: 1988–1994. *J Zoo Wildl Med* **29**, 160–164 (1998).
17. Harris, M. C. & Sleeman, J. M. Morbidity and mortality of bald eagles (*Haliaeetus leucocephalus*) and peregrine falcons (*Falco peregrinus*) admitted to the Wildlife Center of Virginia, 1993–2003. *J Zoo Wildl Med* **38**, 62–66, <https://doi.org/10.1638/05-099.1> (2007).
18. Bueno-Padilla, I., Klaus, G., Gardiner, C. H. & Wuenschmann, A. Disseminated mite infection with ocular involvement in a juvenile bald eagle (*Haliaeetus leucocephalus*). *Vet Ophthalmol* **15**, 271–275, <https://doi.org/10.1111/j.1463-5224.2011.00978.x> (2012).
19. Justice-Allen, A. *et al.* Bald eagle nesting mortality associated with *Argas radiatus* and *Argas ricei* tick infestation and successful management with nest removal in Arizona, USA. *J Wildl Dis* **52**, 940–944, <https://doi.org/10.7589/2015-10-271> (2016).
20. Crozier, B. U. A new taenid cestode, *Cladotaenia banghami*, from a bald eagle. *Trans Am Microsc Soc* **65**, 222–227 (1946).
21. Kocan, A. A. & Locke, L. N. Some helminth parasites of the American bald eagle. *J Wildl Dis* **10**, 8–10 (1974).
22. Smith, H. J. *Cryptocotyle lingua* infection in a bald eagle (*Haliaeetus leucocephalus*). *J Wildl Dis* **14**, 163–164 (1978).
23. Tuggle, B. N. & Schmeling, S. K. Parasites of the bald eagle (*Haliaeetus leucocephalus*) of North America. *J Wildl Dis* **18**, 501–506 (1982).
24. Richardson, D. J. & Cole, R. A. Acanthocephala of the bald eagle (*Haliaeetus leucocephalus*) in North America. *J Parasitol* **83**, 540–541 (1997).
25. Coon, N. C. & Locke, L. N. Aspergillosis in a bald eagle (*Haliaeetus leucocephalus*). *Wildl Dis* **4**, 51 (1968).
26. McAllister, C. T., Duszynski, D. W. & McKown, R. D. A new species of *Caryospora* (Apicomplexa: Eimeriidae) from the bald eagle, *Haliaeetus leucocephalus* (Accipitriformes: Accipitridae), from Kansas. *J Parasitol* **99**, 287–289, <https://doi.org/10.1645/GE-3236.1> (2013).
27. Szabo, K. A., Mense, M. G., Lipscomb, T. P., Felix, K. J. & Dubey, J. P. Fatal toxoplasmosis in a bald eagle (*Haliaeetus leucocephalus*). *J Parasitol* **90**, 907–908, <https://doi.org/10.1645/GE-270R> (2004).
28. Dubey, J. P. *et al.* Genetic characterisation of *Toxoplasma gondii* in wildlife from North America revealed widespread and high prevalence of the fourth clonal type. *Int J Parasitol* **41**, 1139–1147, <https://doi.org/10.1016/j.ijpara.2011.06.005> (2011).
29. Love, D., Kwok, O. C., Verma, S. K., Dubey, J. P. & Bellah, J. Antibody prevalence and isolation of viable *Toxoplasma gondii* from raptors in the Southeastern USA. *J Wildl Dis* **52**, 653–656, <https://doi.org/10.7589/2015-10-269> (2016).
30. Crawley, R. R., Ernst, J. V. & Milton, J. L. Sarcocystis in a bald eagle (*Haliaeetus leucocephalus*). *J Wildl Dis* **18**, 253–255 (1982).
31. Lindsay, D. S. & Blagburn, B. L. Prevalence of encysted apicomplexans in muscles of raptors. *Vet Parasitol* **80**, 341–344 (1999).
32. Olson, E. J., Wunschmann, A. & Dubey, J. P. *Sarcocystis* sp.-associated meningoencephalitis in a bald eagle (*Haliaeetus leucocephalus*). *J Vet Diagn Invest* **19**, 564–568, <https://doi.org/10.1177/104063870701900519> (2007).
33. Stuhlt, J. N., Bowerman, W. W. & Best, D. A. Leucocytozoonosis in nestling bald eagles in Michigan and Minnesota. *J Wildl Dis* **35**, 608–612, <https://doi.org/10.7589/0090-3558-35.3.608> (1999).
34. Greiner, E. C., Black, D. J. & Iverson, W. O. *Plasmodium* in a bald eagle (*Haliaeetus leucocephalus*) in Florida. *J Wildl Dis* **17**, 555–558 (1981).
35. Telford, S. R. Jr., Nayar, J. K., Foster, G. W. & Knight, J. W. *Plasmodium forresteri* n. sp., from raptors in Florida and southern Georgia: its distinction from *Plasmodium elongatum* morphologically within and among host species and by vector susceptibility. *J Parasitol* **83**, 932–937 (1997).
36. Nayar, J. K., Knight, J. W. & Telford, S. R. Jr. Vector ability of mosquitoes for isolates of *Plasmodium elongatum* from raptors in Florida. *J Parasitol* **84**, 542–546 (1998).
37. Windingstad, R. M., Kerr, S. M., Duncan, R. M. & Brand, C. J. Characterization of an avian cholera epizootic in wild birds in western Nebraska. *Avian Dis* **32**, 124–131 (1988).
38. Hoenerhoff, M. *et al.* Mycobacteriosis in an American bald eagle (*Haliaeetus leucocephalus*). *Avian Dis* **48**, 437–441, <https://doi.org/10.1637/7133> (2004).
39. Heatley, J. J. *et al.* Disseminated mycobacteriosis in a bald eagle (*Haliaeetus leucocephalus*). *J Avian Med Surg* **21**, 201–209, doi:10.1647/1082-6742(2007)21[201:DMIABE]2.0.CO;2 (2007).
40. Kelly-Clark, W. K., McBurney, S., Forzan, M. J., Desmarchelier, M. & Greenwood, S. J. Detection and characterization of a *Trichomonas* isolate from a rehabilitated bald eagle (*Haliaeetus leucocephalus*). *J Zoo Wildl Med* **44**, 1123–1126, <https://doi.org/10.1638/2013-0085R.1> (2013).
41. Jessup, D. A. Valvular endocarditis and bacteremia in a bald eagle. *Mod Vet Pract* **61**, 49–51 (1980).
42. Locke, L. N., Lamont, T. G. & Harrington, R. Jr. Isolation of *Streptococcus zooepidemicus* from a bald eagle (*Haliaeetus leucocephalus*). *Avian Dis* **28**, 514–516 (1984).
43. Wilson, M. A., Duncan, R. M., Nordholm, G. E. & Berlowski, B. M. Serotypes and DNA fingerprint profiles of *Pasteurella multocida* isolated from raptors. *Avian Dis* **39**, 94–99 (1995).
44. Stephen, A. A., Leone, A. M., Toplon, D. E., Archer, L. L. & Wellehan, J. F. Jr. Characterization of an *Avipoxvirus* from a bald eagle (*Haliaeetus leucocephalus*) using novel consensus PCR Protocols for the *rpo147* and DNA-dependent DNA polymerase genes. *J Avian Med Surg* **30**, 378–385, <https://doi.org/10.1647/2015-120> (2016).
45. Docherty, D. E., Romaine, R. I. & Knight, R. L. Isolation of a herpesvirus from a bald eagle nestling. *Avian Dis* **27**, 1162–1165 (1983).
46. Goyal, S. M. *et al.* Isolation of mixed subtypes of influenza A virus from a bald eagle (*Haliaeetus leucocephalus*). *Virology* **7**, 174, <https://doi.org/10.1186/1743-422X-7-174> (2010).
47. Redig, P. T. & Goyal, S. M. Serologic evidence of exposure of raptors to influenza A virus. *Avian Dis* **56**, 411–413, <https://doi.org/10.1637/9909-083111-ResNote.1> (2012).
48. Jindal, N., Chander, Y., Primus, A., Redig, P. T. & Goyal, S. M. Isolation and molecular characterization of Newcastle disease viruses from raptors. *Avian pathology: journal of the W.V.P.A* **39**, 441–445, <https://doi.org/10.1080/03079457.2010.517249> (2010).
49. Oliver, J. *et al.* Geography and timing of cases of eastern equine encephalitis in New York State from 1992 to 2012. *Vector Borne Zoonotic Dis* **16**, 283–289, <https://doi.org/10.1089/vbz.2015.1864> (2016).
50. McLaughlin, G. S. *et al.* In *Proceedings of the Joint Conference of the American Association of Zoo Veterinarians, American Association of Wildlife Veterinarians, and Wildlife Disease Association: health and conservation of captive and free-ranging wildlife*. 312–313 (American Association of Zoo Veterinarians).
51. Ray, S. C., Bailey, J. R. & Thomas, D. L. In *Fields Virology*, 6th edition Vol. Volume 1 (eds D.M. Knipe *et al.*) 795–824 (Wolters Kluwer Health/Lippincott Williams & Wilkins, 2013).
52. Chu, L., Jin, M., Feng, C., Wang, X. & Zhang, D. A highly divergent hepacivirus-like flavivirus in domestic ducks. *J Gen Virol* **100**, 1234–1240, <https://doi.org/10.1099/jgv.0.001298> (2019).

53. Lauck, M. *et al.* A novel hepacivirus with an unusually long and intrinsically disordered NS5A protein in a wild Old World primate. *J Virol* **87**, 8971–8981, <https://doi.org/10.1128/JVI.00888-13> (2013).
54. Hartlage, A. S., Cullen, J. M. & Kapoor, A. The strange, expanding world of animal hepaciviruses. *Annual review of virology* **3**, 53–75, <https://doi.org/10.1146/annurev-virology-100114-055104> (2016).
55. Kapoor, A. *et al.* Virome analysis of transfusion recipients reveals a novel human virus that shares genomic features with hepaciviruses and pegiviruses. *MBio* **6**, e01466–01415 (2015).
56. Kapoor, A. *et al.* Identification of rodent homologs of hepatitis C virus and pegiviruses. *MBio* **4**, e00216–00213, <https://doi.org/10.1128/mBio.00216-13> (2013).
57. Beales, L. P., Holzenburg, A. & Rowlands, D. J. Viral internal ribosome entry site structures segregate into two distinct morphologies. *J Virol* **77**, 6574–6579 (2003).
58. Stamatakis, A., Auch, A. F., Meier-Kolthoff, J. & Goker, M. AxPcoords & parallel AxParafit: statistical co-phylogenetic analyses on thousands of taxa. *BMC Bioinformatics* **8**, 405, <https://doi.org/10.1186/1471-2105-8-405> (2007).
59. Li, S. *et al.* Genomic signatures of near-extinction and rebirth of the crested ibis and other endangered bird species. *Genome Biol* **15**, 557, <https://doi.org/10.1186/s13059-014-0557-1> (2014).
60. Spalding, M. G., Kollias, G. V., Mays, M. B., Page, C. D. & Brown, M. G. Hepatic encephalopathy associated with hemochromatosis in a toco toucan. *J Am Vet Med Assoc* **189**, 1122–1123 (1986).
61. Gow, A. G. Hepatic encephalopathy. *Vet Clin North Am Small Anim Pract* **47**, 585–599, <https://doi.org/10.1016/j.cvs.2016.11.008> (2017).
62. Lima, L. C. D., Miranda, A. S., Ferreira, R. N., Rachid, M. A. & Simoes, E. S. A. C. Hepatic encephalopathy: lessons from preclinical studies. *World J Hepatol* **11**, 173–185, <https://doi.org/10.4254/wjh.v11.i2.173> (2019).
63. Dhingra, S., Ward, S. C. & Thung, S. N. Liver pathology of hepatitis C, beyond grading and staging of the disease. *World journal of gastroenterology: WJG* **22**, 1357–1366, <https://doi.org/10.3748/wjg.v22.i4.1357> (2016).
64. Shubin, A. V., Demidyuk, I. V., Komissarov, A. A., Rafieva, L. M. & Kostrov, S. V. Cytoplasmic vacuolization in cell death and survival. *Oncotarget* **7**, 55863–55889, <https://doi.org/10.18632/oncotarget.10150> (2016).
65. Wang, F. *et al.* RNAscope: a novel *in situ* RNA analysis platform for formalin-fixed, paraffin-embedded tissues. *J Mol Diagn* **14**, 22–29, <https://doi.org/10.1016/j.jmoldx.2011.08.002> (2012).
66. Kreuder, C. *et al.* Patterns of mortality in southern sea otters (*Enhydra lutris nereis*) from 1998–2001. *J Wildl Dis* **39**, 495–509, <https://doi.org/10.7589/0090-3558-39.3.495> (2003).
67. Thompson, R. C., Kutz, S. J. & Smith, A. Parasite zoonoses and wildlife: emerging issues. *International journal of environmental research and public health* **6**, 678–693, <https://doi.org/10.3390/ijerph6020678> (2009).
68. Holland, J. *et al.* Rapid evolution of RNA genomes. *Science* **215**, 1577–1585 (1982).
69. Brown, B. T. Winter foraging ecology of bald eagles in Arizona. *The Condor* **95**, 132–138 (1993).
70. Watson, J. W., Garrett, M. G. & Anthony, R. G. Foraging ecology of bald eagles in the Columbia River estuary. *Journal of Wildlife Management* **55**, 492–499 (1991).
71. Knight, R. L. & Skagen, S. K. Agonistic asymmetries and the foraging ecology of bald eagles. *Ecology* **69**, 1188–1194 (1988).
72. Simmonds, P. *et al.* ICTV virus taxonomy profile: *Flaviviridae*. *J Gen Virol* **98**, 2–3, <https://doi.org/10.1099/jgv.0.000672> (2017).
73. Pierson, T. C. & Diamond, M. S. In *Fields Virology*, 6th edition Vol. Volume 1 (eds D.M. Knipe *et al.*) 747–794 (Wolters Kluwer Health/Lippincott Williams & Wilkins, 2013).
74. Tautz, N., Tews, B. A. & Meyers, G. The molecular biology of pestiviruses. *Adv Virus Res* **93**, 47–160, <https://doi.org/10.1016/bs.aivir.2015.03.002> (2015).
75. Smith, D. B. *et al.* Proposed update to the taxonomy of the genera *Hepacivirus* and *Pegivirus* within the *Flaviviridae* family. *J Gen Virol* **97**, 2894–2907, <https://doi.org/10.1099/jgv.0.000612> (2016).
76. Stapleton, J., Fong, S., Muerhoff, A., Bukh, J. & Simmonds, P. The GB viruses: a review and proposed classification of GBV-A, GBV-C (HGV), and GBV-D in genus *Pegivirus* within the family *Flaviviridae*. *J Gen Virol* **92**, 233–246, <https://doi.org/10.1099/vir.0.027490-0> (2011).
77. Tomlinson, J. E. *et al.* Viral testing of 10 cases of Theiler's disease and 37 in-contact horses in the absence of equine biologic product administration: A prospective study (2014–2018). *J Vet Intern Med* **33**, 258–265, <https://doi.org/10.1111/jvim.15362> (2019).
78. Bhattarai, N. & Stapleton, J. T. GB virus C: the good boy virus. *Trends Microbiol* **20**, 124–130, <https://doi.org/10.1016/j.tim.2012.01.004> (2012).
79. Lauck, M. *et al.* GB virus C coinfections in west African Ebola patients. *J Virol* **89**, 2425–2429, <https://doi.org/10.1128/JVI.02752-14> (2015).
80. Pfaender, S., Brown, R. J. P., Pietschmann, T. & Steinmann, E. Natural reservoirs for homologs of hepatitis C virus. *Emerging Microbes and Infections* **3**, e21, <https://doi.org/10.1038/emi.2014.1019> (2014).
81. Scheel, T. K., Simmonds, P. & Kapoor, A. Surveying the global virome: identification and characterization of HCV-related animal hepaciviruses. *Antiviral Res* **115**, 83–93, <https://doi.org/10.1016/j.antiviral.2014.12.014> (2015).
82. Shi, M. *et al.* The evolutionary history of vertebrate RNA viruses. *Nature* **556**, 197–202, <https://doi.org/10.1038/s41586-018-0012-7> (2018).
83. Toohey-Kurth, K., Sibley, S. D. & Goldberg, T. L. Metagenomic assessment of adventitious viruses in commercial bovine sera. *Biologicals: journal of the International Association of Biological Standardization* **47**, 64–68, <https://doi.org/10.1016/j.biologicals.2016.10.009> (2017).
84. Sibley, S. D. *et al.* Novel reovirus associated with epidemic mortality in wild largemouth bass (*Micropterus salmoides*). *J Gen Virol* **97**, 2482–2487, <https://doi.org/10.1099/jgv.0.000568> (2016).
85. Lin, L., Fevery, J. & Hiem Yap, S. A novel strand-specific RT-PCR for detection of hepatitis C virus negative-strand RNA (replicative intermediate): evidence of absence or very low level of HCV replication in peripheral blood mononuclear cells. *J Virol Methods* **100**, 97–105 (2002).
86. Salamov, A. A., Nishikawa, T. & Swindells, M. B. Assessing protein coding region integrity in cDNA sequencing projects. *Bioinformatics* **14**, 384–390 (1998).
87. Almagro Armenteros, J. J. *et al.* SignalP 5.0 improves signal peptide predictions using deep neural networks. *Nature biotechnology* **37**, 420–423, <https://doi.org/10.1038/s41587-019-0036-z> (2019).
88. Kolekar, P., Pataskar, A., Kulkarni-Kale, U., Pal, J. & Kulkarni, A. IRESPred: web server for prediction of cellular and viral internal ribosome entry site (IRES). *Scientific reports* **6**, 27436, <https://doi.org/10.1038/srep27436> (2016).
89. Meszaros, B., Simon, I. & Dosztanyi, Z. Prediction of protein binding regions in disordered proteins. *PLoS Comput Biol* **5**, e1000376, <https://doi.org/10.1371/journal.pcbi.1000376> (2009).
90. Dosztanyi, Z., Meszaros, B. & Simon, I. ANCHOR: web server for predicting protein binding regions in disordered proteins. *Bioinformatics* **25**, 2745–2746, <https://doi.org/10.1093/bioinformatics/btp518> (2009).
91. Zuker, M. Mfold web server for nucleic acid folding and hybridization prediction. *Nucleic Acids Res* **31**, 3406–3415, <https://doi.org/10.1093/nar/gkg595> (2003).
92. Gruber, A. R., Lorenz, R., Bernhart, S. H., Neubock, R. & Hofacker, I. L. The Vienna RNA websuite. *Nucleic Acids Res* **36**, W70–74, <https://doi.org/10.1093/nar/gkn188> (2008).
93. Lorenz, R. *et al.* ViennaRNA Package 2.0. *Algorithms Mol Biol* **6**, 26, <https://doi.org/10.1186/1748-7188-6-26> (2011).

94. Loytynoja, A. Phylogeny-aware alignment with PRANK. *Methods Mol Biol* **1079**, 155–170, https://doi.org/10.1007/978-1-62703-646-7_10 (2014).
95. Talavera, G. & Castresana, J. Improvement of phylogenies after removing divergent and ambiguously aligned blocks from protein sequence alignments. *Syst Biol* **56**, 564–577, <https://doi.org/10.1080/10635150701472164> (2007).
96. Castresana, J. Selection of conserved blocks from multiple alignments for their use in phylogenetic analysis. *Mol Biol Evol* **17**, 540–552 (2000).
97. Abascal, F., Zardoya, R. & Telford, M. TranslatorX: multiple alignment of nucleotide sequences guided by amino acid translations. *Nucleic Acids Res* **38**, W7–13, <https://doi.org/10.1093/nar/gkq291> (2010).
98. Guindon, S. *et al.* New algorithms and methods to estimate maximum-likelihood phylogenies: assessing the performance of PhyML 3.0. *Syst Biol* **59**, 307–321, <https://doi.org/10.1093/sysbio/syq010> (2010).
99. Lefort, V., Longueville, J. E. & Gascuel, O. SMS: smart model selection in PhyML. *Mol Biol Evol* **34**, 2422–2424, <https://doi.org/10.1093/molbev/msx149> (2017).
100. Rambaut, A. FigTree, v1.4.3. Available from <http://tree.bio.ed.ac.uk/software/figtree/> (2016).
101. Lole, K. *et al.* Full-length human immunodeficiency virus type 1 genomes from subtype C-infected seroconverters in India, with evidence of intersubtype recombination. *J Virol* **73**, 152–160 (1999).
102. Nei, M. *Molecular Evolutionary Genetics*. (Columbia University Press, 1987).
103. Kumar, S., Stecher, G. & Tamura, K. MEGA7: Molecular Evolutionary Genetics Analysis version 7.0 for bigger datasets. *Mol Biol Evol* **33**, 1870–1874 (2016).
104. Geographic Distance Matrix Generator (version 1.2.3) (American Museum of Natural History, Center for Biodiversity and Conservation, Available from http://biodiversityinformatics.amnh.org/open_source/gdmg, Accessed on 2019-04-16).
105. Mantel, N. The detection of disease clustering and a generalized regression approach. *Cancer Res* **27**, 209–220 (1967).
106. Paradis, E., Claude, J. & Strimmer, K. APE: analyses of phylogenetics and evolution in R language. *Bioinformatics* **20**, 289–290 (2004).
107. Huson, D. H. & Scornavacca, C. Dendroscope 3: an interactive tool for rooted phylogenetic trees and networks. *Syst Biol* **61**, 1061–1067, <https://doi.org/10.1093/sysbio/sys062> (2012).
108. Legendre, P., Desdevises, Y. & Bazin, E. A statistical test for host-parasite coevolution. *Syst Biol* **51**, 217–234, <https://doi.org/10.1080/10635150252899734> (2002).
109. Meier-Kolthoff, J. P., Auch, A. F., Huson, D. H. & Goker, M. COPYPAT: cophylogenetic analysis tool. *Bioinformatics* **23**, 898–900, <https://doi.org/10.1093/bioinformatics/btm027> (2007).

Acknowledgements

We thank the U.S. Geological Survey National Wildlife Health Center and the Wisconsin Department of Natural Resources for assistance with all aspects of this project, and we gratefully acknowledge the expertise and contributions of the veterinarians, pathologists, epidemiologists, laboratorians, and technicians who worked on the referenced case reports. We also thank N. Businga (WI DNR) and S. Steinfeldt (NWHC) for assistance with sample acquisition and K. Flynn (UW-Madison) for assistance with laboratory assays. This work was supported by the U.S. Geological Survey (award number G14AC00364) and by the University of Wisconsin-Madison through the John D. MacArthur Professorship Chair. The use of trade, product, or firm names is for descriptive purposes only and does not imply endorsement by the US government.

Author contributions

T.L.G., S.D.S. M.E.P. and C.D.D. performed experiments; T.L.G. and S.D.S. analyzed the data; L.L., L.W., and S.S. collected samples; T.L.G. wrote the manuscript. All authors reviewed and improved the final manuscript.

Competing interests

The authors declare no competing interests.

Additional information

Supplementary information is available for this paper at <https://doi.org/10.1038/s41598-019-50580-8>.

Correspondence and requests for materials should be addressed to T.L.G.

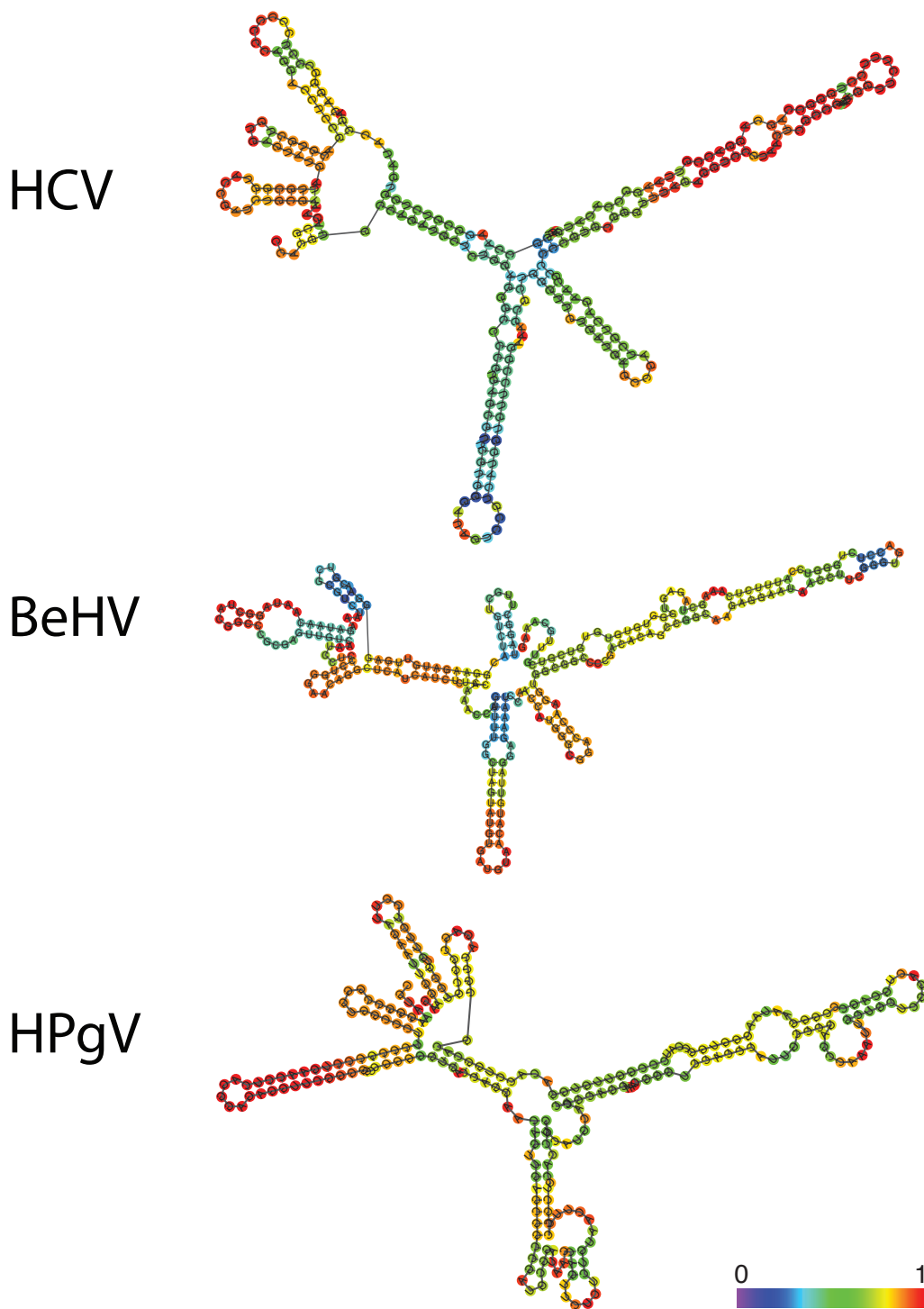
Reprints and permissions information is available at www.nature.com/reprints.

Publisher's note Springer Nature remains neutral with regard to jurisdictional claims in published maps and institutional affiliations.

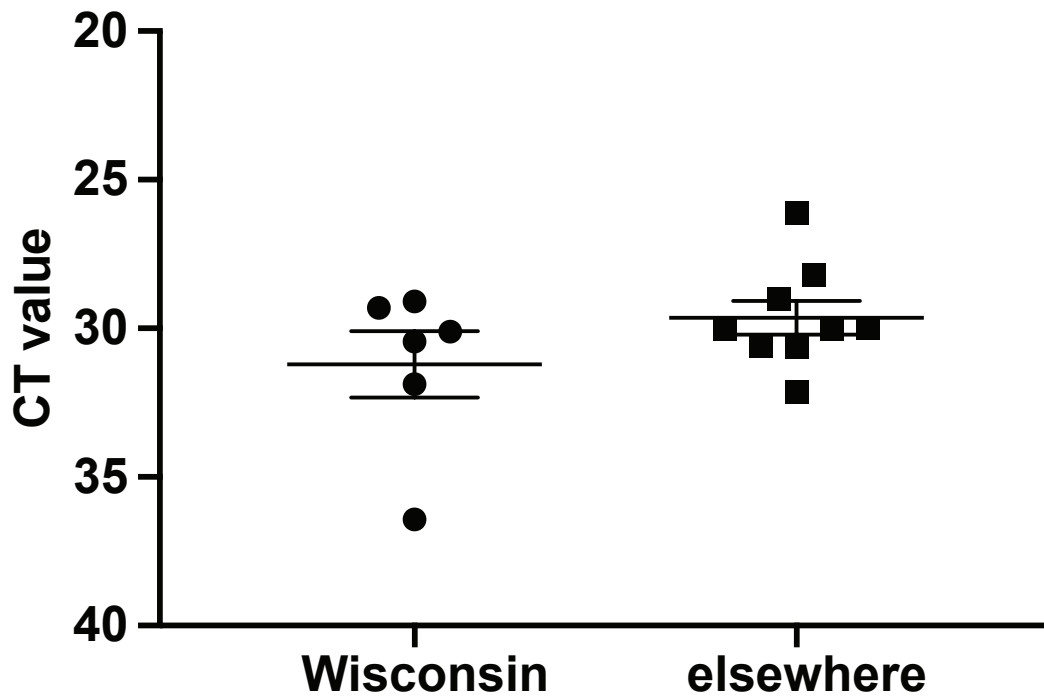


Open Access This article is licensed under a Creative Commons Attribution 4.0 International License, which permits use, sharing, adaptation, distribution and reproduction in any medium or format, as long as you give appropriate credit to the original author(s) and the source, provide a link to the Creative Commons license, and indicate if changes were made. The images or other third party material in this article are included in the article's Creative Commons license, unless indicated otherwise in a credit line to the material. If material is not included in the article's Creative Commons license and your intended use is not permitted by statutory regulation or exceeds the permitted use, you will need to obtain permission directly from the copyright holder. To view a copy of this license, visit <http://creativecommons.org/licenses/by/4.0/>.

© The Author(s) 2019



Supplementary Figure S1: Predicted RNA secondary structures of homologous regions of 5' untranslated regions of hepatitis C virus, genotype 1 (HCV; GenBank accession number NC_004102), bald eagle hepacivirus (BeHV; GenBank accession number MN062427), and the human pegivirus GB virus C (HPgV; GenBank accession number NC_001710). Structures are minimum free energy predictions (-110.12, -87.67, and -118.62 kcal/mol, respectively) generated by the RNAfold algorithm on the Vienna RNA Website server^{92,93}; colored scales indicate base-pair probabilities.



Supplementary Figure S2: Relative loads of bald eagle hepatic virus (BeHV) in bald eagle liver tissues. Ct values are averages across triplicate quantitative real-time reverse transcription PCR assays. Lower Ct values indicate higher relative viral loads, lines indicate means, and error bars indicate standard errors of the mean. Values are shown for six eagles from Wisconsin compared to nine eagles from elsewhere (see Table S1); the difference is not statistically significant ($t=1.376$; $df=13$; $P=0.1920$).

Table S1: Liver samples used for characterization of bald eagles and viruses

<i>Accession</i>	<i>Age</i>	<i>Sex</i>	<i>Date</i>	<i>State</i>	<i>County</i>	<i>Cause of death</i>	<i>BEHV</i>	<i>ID in Figure 3</i>
2006-39	Immature	Female	4/27/06	WI*	Columbia	Electrocution	POS	A
26941	Immature	Male	1/21/16	WI	La Crosse	Enteritis	POS	B
27149	Adult	Female	3/30/16	NE	Webster	Lead poisoning	POS	C
17498	Adult	Female	1/6/02	WI	Grant	Lead poisoning or WRES	POS	D
26985	Adult	Female	2/3/16	KS	Cloud	Trauma: impact	POS	E
26886	Adult	Male	12/8/15	MN	Houston	Lead poisoning	POS	F
18490	Immature	Male	12/29/02	WI*	Sauk	WRES	POS	G
27147	Adult	Female	3/30/16	NE	Buffalo	Trauma	POS	H
26998	Immature	Male	2/10/16	FL	De Soto	Trauma: impact	POS	I
17477	Adult	Female	12/18/01	ND	Sargent	Enteritis	POS	J
19373	Immature	Female	3/9/05	WA	Whatcom	Trauma	POS	K
26529	Adult	Male	5/29/15	WI	Adams	Trauma	POS	L
26778	Adult	Female	9/15/15	WI	Clark	Undetermined	POS	M
26976	Adult	Female	1/29/16	WA	Grays Harbor	Emaciation	POS	N
26856	Adult	Female	11/6/15	WA	Grays Harbor	Drowning	POS	O
18619	Immature	Female	4/22/03	AZ	Coconino	Lead poisoning	neg	n/a
19045	Adult	Male	4/27/04	MD	Dorchester	Trauma	neg	n/a
19227	Adult	Male	9/16/04	VA	Stafford	Gangrene	neg	n/a
19396	Immature	Unknown	4/15/05	MD	Hartford	Trauma	neg	n/a
19762	Immature	Unknown	5/19/06	AZ	Pinal	Trauma	neg	n/a
20129	Immature	Female	1/30/07	AR	Poinsett	Trauma	neg	n/a
20165	Adult	Male	12/30/06	NC	Beaufort	Electrocution	neg	n/a
20341	Adult	Male	7/12/07	OR	Crook	Trauma	neg	n/a
23016	Immature	Male	4/21/10	IL	Calhoun	Aspergillosis	neg	n/a
24668	Adult	Male	1/30/14	WI	Oneida	Emaciation	neg	n/a
26001	Immature	Female	10/7/14	AK	Kodiak Island	Avian pox	neg	n/a
26093	Immature	Male	12/18/14	NJ	Hunterdon	Trauma	neg	n/a
26758	Immature	Male	9/3/15	AK	Valdez-Cordova	Avian pox	neg	n/a
26853	Adult	Male	11/4/15	VA	Prince William	Trauma: gunshot	neg	n/a
26918	Adult	Male	1/4/16	WI	Lafayette	Trauma: gunshot	neg	n/a
26978	Adult	Male	1/29/16	WA	Klickitat	Choking	neg	n/a
26993	Adult	Male	2/5/16	GA	Harris	Trauma: impact	neg	n/a
26999	Adult	Female	2/10/16	NC	Richmond	Trauma: impact	neg	n/a
27005	Adult	Female	2/12/16	SC	Kershaw	Trauma	neg	n/a
27038	Adult	Female	2/24/16	FL	Seminole	Trauma: impact	neg	n/a
27039	Adult	Male	2/24/16	FL	Orange	Trauma	neg	n/a
27040	Adult	Female	2/24/16	FL	Seminole	Trauma: gunshot	neg	n/a
27056	Adult	Male	3/1/16	AZ	Navajo	Lead poisoning	neg	n/a
20165	Adult	Male	12/30/06	NC	Beaufort	Electrocution	neg	n/a
26093	Immature	Male	12/18/14	NJ	Hunterdon	Trauma	neg	n/a
26689	Adult	Female	8/6/15	NE	Clay	Undetermined	neg	n/a
26744	Adult	Male	8/28/15	MD	Kent	Starvation	neg	n/a
26940	Adult	Female	1/20/16	WA	Spokane	Emaciation	neg	n/a
26977	Immature	Female	1/29/16	WA	Grays Harbor	Undetermined	neg	n/a
26982	Adult	Male	2/2/16	MT	Lincoln	Lead poisoning	neg	n/a
26986	Adult	Male	2/3/16	GA	Bryan	Trauma: impact	neg	n/a
27148	Adult	Female	3/30/16	NE	Nuckolls	Electrocution	neg	n/a

* Counties bordering the lower Wisconsin River

Table S2. Oligonucleotide primers and probes used in the study

<i>Name*</i>	<i>Sequence (5'-3')</i>	<i>Amplicon size (bp)</i>
<i>Primers for diagnostic nested PCR of the BeHV NS3 gene</i>		
BEHV-NS3-EX-F3869†	GATGTAGTGCTTTGTGATGAGTGTCA	262
BEHV-NS3-EX-R4084	CCTTTGAACCACAAAAGATGACGTG	
BEHV-NS3-IN-F3918	GCATTGGTACTGTGCTCACG	138
BEHV-NS3-IN-R4017	CCACTTCTCCCTCGTCAGTC	
<i>Primers for nested PCR and sequencing of the BeHV envelope gene ‡</i>		
BEHV-ENV-EX-F491	TCCCTTCTTGTGTGGCTGAT	1550-1676
BEHV-ENV-EX-F525	TCTCGTCAATGGAAGTGGGA	
BEHV-ENV-EX-R2074	GAGCATAAACCCAAGCAAGC	
BEHV-ENV-EX-R2166	AAGGGCTAAAGCAGGGTAGC	
BEHV-ENV-IN-F582	GCTGTCACACATGGAAGTGC	1348-1493
BEHV-ENV-IN-F644	CGGTTCCCTGGTTCATGACT	
BEHV-ENV-IN-R1991	GCTGTCACACATGGAAGTGC	
BEHV-ENV-IN-R2074	GAGCATAAACCCAAGCAAGC	
<i>Primers and probe for real time quantitative PCR of the BeHV envelope gene</i>		
BEHV-QRT-F299	TTTTCCAAGCTCTCGCCGATAG	146
BEHV-QRT-R444	CCTACCAGCAGCTAGATAGAGTATGA	
BEHV-QRT-PRB	/56-FAM/CACTGTTCC/ZEN/AATAGGCTTGTTTAGGTTGATTG/3IABkFQ/	

*Numbers included in primer names indicate the nucleotide position to which the 5' base of each primer anneals within the BeHV polyprotein open reading frame.

†This primer was appended with tag sequence 5'-AAGCAGTGGTATCAACGCAGAGT-3' during negative strand PCR to assess of viral replication; see text for details.

‡Various combinations of external and internal primers were used to obtain envelope gene sequences from all BeHV-positive tissues.

Table S3: Viruses used in phylogenetic analysis of complete polyprotein genes

<i>Virus</i>	<i>Abbreviation</i>	<i>Isolate</i>	<i>Genus</i>	<i>Host</i>	<i>Country</i>	<i>Year</i>	<i>Accession</i>
Bald eagle hepatitis virus	BeHV	NA03-001	Hepacivirus	Bald eagle (<i>Haliaeetus leucocephalus</i>)	USA	2002	MN062427
Bat hepatitis virus A	BHVA	PDB-112	Hepacivirus	Striped leaf-nosed bat (<i>Hipposideros vittatus</i>)	Kenya	2010	NC_031916
Bat hepatitis virus C	BHVC	PDB-452	Hepacivirus	Large-eared free-tailed bat (<i>Otomops martiensseni</i>)	Kenya	2010	NC_031947
Bovine hepatitis virus	BOHV	GHC25	Hepacivirus	Cow (<i>Bos taurus</i>)	Ghana	2011	NC_026797
Chinese broad-headed pond turtle hepatitis virus	CBHP/THV	WHWGGF64311	Hepacivirus	Chinese broad-headed pond turtle (<i>Chinemys megalocephala</i>)	China	unspecified	MG600000
Duck hepatitis virus	DuHV	HCL-1	Hepacivirus	Domestic duck (<i>Anas platyrhynchos domestica</i>)	China	2018	MK737639
Equine hepatitis virus	EQHV	JPN3	Hepacivirus	Horse (<i>Equus caballus</i>)	Japan	2013	NC_024889
GB virus B	GBVB	XXX	Hepacivirus	Moustached tamarin (<i>Saguinus mystax</i>)	unknown	<1995	NC_001655
Guangxi chinese leopard gecko hepatitis virus	GCLGHV	PXJHG3419	Hepacivirus	Chinese leopard gecko (<i>Goniurosaurus luii</i>)	China	unspecified	MG599988
Guangxi houndshark hepatitis virus	GHHVa	NHJSG30635	Hepacivirus	Starspotted smooth-hound houndshark (<i>Mustelus manazo</i>)	China	unspecified	MG599994
Guangxi houndshark hepatitis virus	GHHVb	RBCSG7845	Hepacivirus	Starspotted smooth-hound houndshark (<i>Mustelus manazo</i>)	China	unspecified	MG599998
Guereza hepatitis virus	GHV	BWC05	Hepacivirus	Black-and-white colobus monkey (<i>Colobus guereza</i>)	Uganda	2010	KC551801
Hepatitis C virus 1	HCV1	H77	Hepacivirus	Human (<i>Homo sapiens</i>)	United States	1977	NC_004102
Hepatitis C virus 2	HCV2	HC-J6CH	Hepacivirus	Human (<i>Homo sapiens</i>)	Japan	unspecified	NC_009823
Hepatitis C virus 3	HCV3	NZL1	Hepacivirus	Human (<i>Homo sapiens</i>)	New Zealand	unspecified	NC_009824
Hepatitis C virus 4	HCV4	ED43	Hepacivirus	Human (<i>Homo sapiens</i>)	Egypt	unspecified	NC_009825
Hepatitis C virus 5	HCV5	EUH1480	Hepacivirus	Human (<i>Homo sapiens</i>)	United Kingdom	unspecified	NC_009826
Hepatitis C virus 6	HCV6	Th580	Hepacivirus	Human (<i>Homo sapiens</i>)	Thailand	unspecified	NC_009827
Hepatitis C virus 7	HCV7	QC69	Hepacivirus	Human (<i>Homo sapiens</i>)	DR Congo	2002	EF108306
Nanhai dogfish shark hepatitis virus	NDSHV	NHJSG30261	Hepacivirus	Japanese shortnose spurdog shark (<i>Squalus brevirostris</i>)	China	unspecified	MG599995
Nanhai ghost shark hepatitis virus 2	NGSHV2	NHYJG60710	Hepacivirus	Ghost shark (<i>Chimaera</i> sp.)	China	unspecified	MG599997
Non-primatae hepatitis virus	NPHV	AAK-2011	Hepacivirus	Domestic dog (<i>Canis lupus familiaris</i>)	USA	2011	JF744991
Norway rat hepatitis virus	NRHV	NYC-E43	Hepacivirus	Norway rat (<i>Rattus norvegicus</i>)	USA	2012	NC_025673
Rodent hepatitis virus	RHV	RHV-339	Hepacivirus	Deer mouse (<i>Peromyscus maniculatus</i>)	USA	2008	NC_021153
Sigmodontinae hepatitis virus	SIHV	Om/2012	Hepacivirus	Black-footed pygmy rice rat (<i>Oligoryzomys nigripes</i>)	Brazil	2012	MH370348
Wenling shark virus	WLSV	MHS-2	Hepacivirus	Graceful catshark (<i>Proscyllium habereri</i>)	China	2014	KR902729
Western African lungfish hepatitis virus	WALHV	FZFYG124617	Hepacivirus	West African lungfish (<i>Protopterus annectens</i>)	Nigeria	unspecified	MG599993
Xiamen guitarfish hepatitis virus	XGHV	BWLYTG5315	Hepacivirus	Ringstreaked guitarfish (<i>Rhinobatos hynnicephalus</i>)	China	unspecified	MG599991
Xiamen sepioid hepatitis virus	XSSHV	DHHHBHGS10983	Hepacivirus	Sepia stingray (<i>Urolophus aurantiacus</i>)	China	unspecified	MG599992
Yili teratoscincus roborowskii hepatitis virus	YTRHV	YLSHG5584	Hepacivirus	Supreme gecko (<i>Teratoscincus roborowskii</i>)	China	unspecified	MG599987
Bat pegivirus	BPgV1	PDB-694	Pegivirus	Straw-coloured fruit bat (<i>Eidolon helvum</i>)	Nigeria	2010	KC796083
Bat pegivirus	BPgV2	PDB-76.1	Pegivirus	Tomb bat (<i>Taphozous</i> sp.)	Cameroon	2010	KC796084
Bat pegivirus	BPgV3	PDB-838	Pegivirus	Egyptian fruit bat (<i>Roussettus aegyptiacus</i>)	Kenya	2011	KC796086
Bat pegivirus	BPgV4	PDB-1734	Pegivirus	Seba's short-tailed bat (<i>Carollia perspicillata</i>)	Guatemala	2010	KC796087
Bat pegivirus	BPgV5	PDB-1715	Pegivirus	Little yellow-shouldered bat (<i>Sturnira lilium</i>)	Guatemala	2010	KC796088
Bat pegivirus	BPgV6	PDB-491.2	Pegivirus	Large-eared free-tailed bat (<i>Otomops martiensseni</i>)	Kenya	2010	KC796089
Equine pegivirus 1	EQPgV	C0035	Pegivirus	Horse (<i>Equus caballus</i>)	USA	2011	NC_020902
GB virus A	GBVAtri	tri	Pegivirus	Three-striped night monkey (<i>Aotus trivirgatus</i>)	USA	<1996	AF023425
GB virus A	GBVAAlab	Alab	Pegivirus	White-lipped tamarin (<i>Saguinus labianus</i>)	USA	<1996	NC_001837
Human pegivirus (GB virus C)	HPgV	PNF2161	Pegivirus	Human (<i>Homo sapiens</i>)	USA	unspecified	NC_001710
Norway rat pegivirus	NRPgV	NYC-EI3	Pegivirus	Norway rat (<i>Rattus norvegicus</i>)	USA	2012	NC_025679
Rodent pegivirus	RPgV	CC61	Pegivirus	Desert woodrat (<i>Neotoma lepida</i>)	USA	2008	NC_021154
Simian pegivirus (chimpanzee)	SPgVtro	GBV-Ctro	Pegivirus	Chimpanzee (<i>Pan troglodytes</i>)	Japan	<1980	AF070476
Simian pegivirus (red colobus)	SPgV/krc	RC008	Pegivirus	Red colobus monkey (<i>Ptilocolobus tephrosceles</i>)	Uganda	2010	NC_024377
Theiler's disease-associated virus	TDgV	HorseA1_serum	Pegivirus	Horse (<i>Equus caballus</i>)	USA	2011	KC145265